Published in final edited form as:
Structure. 2009 September 9; 17(9): 1156–1168. doi:10.1016/j.str.2009.07.014.

The Nuclear Pore Complex has entered the Atomic Age

Stephen G. Brohawn[†], **James R. Partridge**[†], **James R. R. Whittle**[†], and **Thomas U. Schwartz**[*]
Department of Biology, Massachusetts Institute of Technology 77 Massachusetts Avenue, Cambridge, MA 02139, USA

Abstract

Nuclear pore complexes (NPCs) perforate the nuclear envelope and represent the exclusive passageway into and out of the nucleus of the eukaryotic cell. Apart from their essential transport function, components of the NPC have important, direct roles in nuclear organization and in gene regulation. Due to its central role in cell biology, it is of considerable interest to determine the NPC structure at atomic resolution. The complexity of these large, 40-60 MDa protein assemblies has for decades limited such structural studies. More recently, exploiting the intrinsic modularity of the NPC, structural biologists are making progress toward understanding this nanomachine in molecular detail. Structures of building blocks of the stable, architectural scaffold of the NPC have been solved, and distinct models for their assembly proposed. Here we review the status of the field and lay out the challenges and the next steps toward a full understanding of the NPC at atomic resolution.

Introduction

The hallmark of eukaryotic cells is an elaborate endomembrane system that creates membrane-enclosed organelles. The nucleus is the most prominent organelle, as it harbors the genetic material of the cell. NPCs are the only gateways to the nucleus and reside in circular openings in the nuclear envelope where the inner nuclear membrane (INM) and outer nuclear membrane (ONM) of the nuclear envelope (NE) are fused. NPCs are among the largest multiprotein assemblies in the quiescent cell and were first described 50 years ago by electron microscopy (Watson, 1959). Here we review the status of structural characterization of the nuclear pore complex – the results of truly multi-disciplinary efforts. For general reviews the reader is also referred to (D'Angelo and Hetzer, 2008; Lim et al., 2008; Tran and Wente, 2006) and for the mechanism of NPC assembly to (Antonin et al., 2008) and for nucleocytoplasmic transport of proteins and RNAs to (Carmody and Wente, 2009; Cook et al., 2007; Kohler and Hurt, 2007; Pemberton and Paschal, 2005; Stewart, 2007; Weis, 2003). The role of the NPC in gene regulation and nuclear organization is addressed in (Akhtar and Gasser, 2007; Heessen and Fornerod, 2007).

Overall Structure

Electron microscopy has been the best technique to observe the overall structure of the NPC. A variety of cell types from different organisms have been imaged. In its internal symmetry,

*Correspondence: tus@mit.edu.
[†]the first three authors contributed equally to this work.

shape, and size the NPC seems conserved throughout evolution, though at the molecular level there are differences, as noted below. In internal symmetry, the first electron micrographs of the NPC showed that it forms an octagonal ring whose central channel is less electron dense that the eight lobes that surround it. In shape, scanning electron microscopy experiments (SEM) have recorded some of the most stunning NPC images (Figure 1). While the architectural core is grossly symmetric about the plane of the membrane, the peripheral components on the nuclear and cytoplasmic faces are distinct. These peripheral components recapitulate the eightfold symmetry about the transport axis exhibited by the architectural core. On the cytoplasmic side, eight knobs, thought to be attachment sides for fibrous extensions, are visible in NPCs from multicellular species (Kiseleva et al., 2000). In yeast, these features are less pronounced, but likely are also present (Kiseleva et al., 2004). On the nucleoplasmic side, a ring termed the nuclear basket is suspended from eight filaments that join it to the NPC. Lastly, in size, the diameter of the NPC appears to be similar in all eukaryotes, about 90-120nm (Akey and Radermacher, 1993;Beck et al., 2007;Fahrenkrog et al., 2000;Hinshaw et al., 1992;Stoffler et al., 2003). However, there is still considerable uncertainty about the height, determined to be ~30-50nm (Alber et al., 2007b;Elad et al., 2009).

Further work has led to progressively more detailed reconstructions of the NPC. Cryo-electron microscopy that relies on averaging images from many NPCs has been employed to study the core NPC structure, the part that spans the distance between the faces of INM and ONM (Akey and Radermacher, 1993; Hinshaw et al., 1992). These studies have shown that the scaffold ring structure – the electron dense material near the nuclear membrane – has alternating thicker and thinner regions, hence it is often called the spoke ring (Akey and Radermacher, 1993; Hinshaw et al., 1992). The scaffold structure appears to penetrate the pore membrane to also form a perinuclear ring structure. Using cryo-electron tomography, the best pictures of complete NPCs have been achieved, extending even to a resolution of ~ 6 nm (Beck et al., 2007; Elad et al., 2009). With this technique, details of the ring structures become apparent. The scaffold can be divided into three main ring elements: a central spoke ring is sandwiched between a cytoplasmic ring and a nucleoplasmic ring. The rings appear to float on top of one another, indicating that material connecting them is less electron-dense than the rings themselves. Alternatively, this may be due to technical difficulties, such as the ‘missing cone’ problem or poor resolution in the Z-direction.

The central transport cavity of the nuclear pore complex shows no distinct structural features, consistent with the perception that it is filled by an aqueous meshwork formed by natively unfolded FG-domains, which are long polypeptide sequences found in several nucleoporins that contain phenylalanine-glycine (FG) repeats but are otherwise hydrophilic. These extensions are thought to form a distinct, semi-permeable environment that prevents the diffusion of large molecules, unless they are bound to nuclear transport factors that facilitate entry into this central cavity.

In addition to the central channel, the scaffold itself likely harbors additional, peripheral channels. The spoke ring appears porous in cryo-EM/-ET structures, with gaps of ~ 9 nm diameter close to the NE membrane (Hinshaw et al., 1992; Stoffler et al., 2003). Peripheral channels have been discussed in several studies, and postulated to transport small proteins and ions (Kramer et al., 2007). It is unclear, however, how this type of transport could be restricted to the peripheral channels, when the central channel could allow it as well. Alternatively, it also has been suggested that the peripheral channels transport membrane proteins destined for the INM. These are inserted into the ER membrane following translation and stay membrane-anchored until they reach their final destination (the ER, ONM, and INM are all contiguous). Perhaps these membrane proteins pass the NPC into the nucleus via these peripheral channels (Powell and Burke, 1990; Zuleger et al., 2008). The nucleoplasmic domains of INM proteins are limited in size to ~ 40 kDa, about as large as cavities of the observed channels.

While the general NPC architecture is well established, the cryo-EM/-ET structures do not permit the assignment of individual proteins, since their boundaries are not visible at this resolution. For this, higher resolution methods are required.

Modularity

A characteristic of the NPC is its high degree of modularity, which manifests itself at several levels. First, the NPC is organized around a central eightfold rotational symmetry. Second, only ~30 nucleoporins, composed of a limited set of domain topologies, build the NPC. Third, nucleoporins have various dwell times at the NPC, with only a fraction being stably attached at all times. And finally, the stably attached nucleoporins are arranged into subcomplexes, each of which assembles in multiple copies to build the entire NPC (Figure 2). This modularity is the basis for approaching structural determination of the assembly at atomic resolution (Schwartz, 2005).

Protein Composition

Two studies, using *S. cerevisiae* (Rout et al., 2000) and rat hepatocytes (Cronshaw et al., 2002) as starting material, determined an inventory of nucleoporins. In both studies, cell extracts were enriched for NPCs by fractionation and analyzed by mass-spectrometry to identify the proteins purified thereby. The set of proteins found in both organisms is largely identical and comprises ~ 30 different gene products. The nucleoporins can be broadly classified into three categories (Figure 3). ~10 contain disordered N- and/or C-terminal regions that are rich in phenylalanine-glycine (FG) repeats. These FG-repeat regions emanate into and form the transport barrier in the channel of the NPC. ~15 nucleoporins have a distinct architectural functions and form the NPC scaffold structure. Three nucleoporins have transmembrane domains and anchor the NPC in the circular openings in the NE. Immunogold-labeling of all nucleoporins shows that the majority of the nups, notably scaffold nucleoporins, are symmetrically localized around a two-fold symmetry axis in the plane of the NE, perpendicular to the eightfold rotational symmetry about the main transport channel (Rout et al., 2000). Based on simple hydrodynamic and volumetric calculations the size of the NPC was estimated to range from 66 MDa in *S. cerevisiae* (Rout and Blobel, 1993) to 125 MDa in vertebrates (Reichelt et al., 1990). Calculations based on the stoichiometry of nucleoporins obtained in the proteomic studies, however, indicate that the NPC size is only 44 MDa in *S. cerevisiae* and ~ 60 MDa in rat. The discrepancy supports the conclusion that the NPC is a porous, lattice-like assembly, rather than a solid entity (Brohawn et al., 2008; Hinshaw et al., 1992), which accounts for the overestimate of mass based on volumetric analysis.

Subcomplexes

The majority of nucleoporins are organized in discrete subcomplexes each present in multiple copies that arrange according to the symmetry elements of the NPC to form the complete structure. The subcomplexes are biochemically defined and reflect the stable interaction of subsets of nucleoporins. Interestingly, these subcomplexes are also found as entities in mitotic extracts of higher eukaryotes, when the nuclear envelope breaks down during open mitosis (Matsuoka et al., 1999). At the end of mitosis, NPCs reassemble from these subcomplexes in a defined order (Dultz et al., 2008). Each of the eight spokes arranged around the central rotational axis is composed of 5 subcomplexes (Figure 2). Nup82/Nup159/Nsp1 form a subcomplex localized at the cytoplasmic side of the NPC (Belgareh et al., 1998). A second pool of Nsp1 complexes with Nup57 and Nup49 and resides in the center of the NPC, forming the bulk of the central transport barrier (Grandi et al., 1993). The scaffold ring is constructed from two major subcomplexes: the heptameric Y- or Nup84-complex and the heteromeric Nic96 complex. The Y-complex is the best-characterized subcomplex of the NPC and is essential for its assembly, as shown in several organisms (Boehmer et al., 2003; Fabre and

Hurt, 1997; Galy et al., 2003; Harel et al., 2003; Walther et al., 2003). It has 7 universally conserved components – Nup84, Nup85, Nup120, Nup133, Nup145C, Sec13 and Seh1 – that assemble stoichiometrically and exhibit the eponymous Y-shape in electron micrographs (Kampmann and Blobel, 2009; Lutzmann et al., 2002; Siniossoglou et al., 2000). In many eukaryotes, notably excluding *S. cerevisiae*, three additional proteins, Nup37, Nup43, and ELYS/MEL-28, are considered members of the Y-complex, but their architectural role is unclear (Cronshaw et al., 2002; Franz et al., 2007; Rasala et al., 2006). In most models, the Y-complex is thought to symmetrically localize to the cytoplasmic and the nucleoplasmic face of the NPC sandwiching the Nic96 complex. The Nic96 complex is not as well defined as the Y-complex, likely reflecting the fact that it associates less stably. However, Nic96 interacts directly with Nup53/59 (Hawryluk-Gara et al., 2005), and co-immunoprecipitation with Nup188 (Nehrbass et al., 1996) and with Nup192 have been reported (Kosova et al., 1999). Further, the Nic96 complex is the tether to the Nsp1 complex in the center of the NPC. The newest defined subcomplex contains the transmembrane Nup Ndc1, considered to be an anchor for the NPC in the pore membrane. This complex contains Nup157/170 and Nup53/59, which connect the Ndc1 complex to the Nic96 complex (Makio et al., 2009; Onischenko et al., 2009). The other two transmembrane nups, Pom34 and Pom152, are reported to interact with Ndc1 as well, albeit less strongly. Mlp1/2 are attached to the NPC ring via Nup60 (Feuerbach et al., 2002) and likely form the nuclear basket structure (Strambio-de-Castillia et al., 1999) .

Dynamics

An important aspect of the NPC is that it is not a rigidly assembled machine, but a rather dynamic entity. Inverse fluorescence recovery after photobleaching experiments using GFP-tagged nucleoporins showed that different parts of the NPC have drastically different residence times (Rabut et al., 2004). Some mobile components detach from the NPC within seconds, while other components are stable throughout the entire cell cycle. Notably, the components of the structural scaffold – the Y-complex and the Nic96 complex – are stably attached, while FG-nucleoporins are more dynamic. These studies on nucleoporin dynamics are consistent with the very slow protein turnover of scaffold nucleoporins (D'Angelo et al., 2009; Daigle et al., 2001). The scaffold structure of the NPC can be viewed as a docking site for more mobile nucleoporins, which often have functional roles at sites away from the NPC (Kalverda and Fornerod, 2007).

Domain Architecture

Until about five years ago, very little high-resolution structural information on nucleoporins was available. This was largely due to the technical difficulties of obtaining nucleoporins of sufficient quantity and quality for structural studies, a challenge particularly severe in the case of scaffold nucleoporins. Despite the scarcity of experimental evidence, structural predictions grouped nucleoporins into a small set of fold classes (Berke et al., 2004; Devos et al., 2004; Devos et al., 2006; Schwartz, 2005). First, FG-domains, the primary transport factor interaction sites, are present in about one third of all nucleoporins. Second, coiled-coil domains are present in a number of nucleoporins. Third, scaffold nucleoporins are largely composed of β-propellers, α-helical domains, or a tandem combination of both. Using this simple classification, about 76 % of the mass of the yeast NPC was accounted for.

FG-repeats

A total of 13 % of the NPC mass is made up of FG-repeat containing peptide stretches. The repeats are found in terminal extensions of ~10 nucleoporins and make up the physical transport barrier. NTRs specifically interact with the FG-regions, which allow them to enter the central transport channel. How FG-repeat regions exactly form the transport barrier is vigorously investigated, and hotly debated (Frey and Gorlich, 2007; Lim et al., 2007; Peters, 2009; Rout

et al., 2003). Systematic deletion of FG-regions from different nups has shown that the total mass of these filaments is more important than any one individual FG-filament, arguing for substantial redundancy in the meshwork (Terry and Wente, 2007). The intrinsic disorder of the FG-filaments stretches is well documented in a series of crystal structures (Bayliss et al., 2000; Fribourg et al., 2001; Grant et al., 2003; Liu and Stewart, 2005). Only short peptide stretches are orderly bound to the convex outer surface of the HEAT-repeats that build NTRs, with the phenylalanine sidechains inserting between neighboring helices. Otherwise, the filaments remain without structure. Little is known about the intervening, non-FG sequences. They are poorly conserved, but are rich in polar and charged residues, probably important for the biophysical properties of the transport barrier.

Coiled-coils

Coiled coils in the NPC fulfill structural roles. The nuclear basket of the NPC is mainly constructed from the large coiled-coil proteins Mlp-1/2 in yeast and Tpr in vertebrates. Coiled-coils are often used for protein-protein interactions, thus the nuclear basket may serve as a general recruitment platform to bring accessory factors close to the NPC. The desumoylating enzyme Ulp1, for example, is stably associated with the nuclear basket (Li and Hochstrasser, 2000). Lining the central NPC channel are 6 nucleoporins containing coiled-coil regions. The FG-Nup Nsp1 is part of two distinct entities, the Nsp1-Nup57-Nup49 complex (Grandi et al., 1993) and the Nsp1-Nup82-Nup159 complex (Bailer et al., 2001). In both, the proteins are held together by coiled-coil interactions (Bailer et al., 2001) and the Nsp1-Nup57-Nup49 complex is, in addition, tethered to the NPC scaffold via the N-terminal coiled-coil region of Nic96 (Grandi et al., 1995). So far, only a homodimerized 10 kDa fragment of Nup58 (the vertebrate ortholog to Nup57) has been structurally characterized (Melcak et al., 2007). Biochemical analysis suggests that the network involves specific rather than promiscuous interactions, arguing for a specific tethering function for the coiled-coil segments. It will be interesting to see these coiled-coil interactions in atomic detail in order to manipulate them and potentially swap the attached FG-domains within the NPC. Such experiments could provide important insight into the organization of the FG-network, if there is such.

β-Propellers

A large portion of the NPC scaffold is build from β-propellers, one of the most abundant classes of proteins, especially in eukaryotes, and with diverse functions (Chaudhuri et al., 2008; Paoli, 2001). A set of Nups were initially identified as β-propellers based on sequence analysis. In yeast, only Sec13 and Seh1 contain the signature WD-40 repeat motif and were among the very first β-propellers to be recognized (Pryer et al., 1993). More nups have since been recognized as β-propellers despite the lack of signature sequence motifs. The N-terminal domain of Nup133 was the first experimentally determined β-propeller of the NPC and after this structure was solved, the additional non-canonical β-propeller domains in the NPC were identified (Berke et al., 2004). To date, 5 of the 8 universally conserved β-propellers in the NPC are structurally characterized (Figure 4). In Nup133, Nup120, and Nup159 (hNup214) the β-propellers are N-terminal and seven-bladed. While forming a distinct entity in Nup133 and Nup159 (Weirich et al., 2004), physically tethered but otherwise not interacting strongly with the C-terminal part of the protein, the β-propeller in Nup120 is fully integrated with an adjacent helical domain to build one continuous oblong domain (Leksa et al., 2009). Seh1 and Sec13 are so far unique variations of β-propellers in that they are open and 6-bladed (Brohawn et al., 2008; Debler et al., 2008; Fath et al., 2007; Hsia et al., 2007). Their partner proteins insert a seventh blade into the β-propeller to complete the domain *in trans*. The function of the β-propellers is architectural and it is widely assumed that they serve as protein-protein interaction sites. Peripheral β-propellers can recruit accessory proteins, like the mRNA export

factor Dbp5 (von Moeller et al., 2009), whereas those more centrally located likely are used to connect subcomplexes.

α-Helical Domains

α-Helical domains make up more than half of the mass of the NPC scaffold. Structural prediction classified the non-coiled-coil α-helical domains into a strongly related group of α-helical solenoids (Devos et al., 2006). α-solenoids are characterized by a two or three helix unit that is repeatedly stacked to form an elongated, often superhelical domain with N and C terminus at opposite ends of the molecule (Kobe and Kajava, 2000). Such regular, α-helical repeat structures are, often in combination with β-propellers, common scaffolds in large protein assemblies such as the clathrin vesicle coat (Edeling et al., 2006), the protein phosphatase 2A holoenzyme (Xu et al., 2006) and the anaphase promoting complex (Herzog et al., 2009), to name a few. Surprisingly, structural characterization of α-helical domain containing Nups has revealed three different α-helical folds, each distinct from a regular α-solenoid arrangement (Boehmer et al., 2008; Jeudy and Schwartz, 2007; Leksa et al., 2009; Schrader et al., 2008b). Nic96 was the first experimentally determined α-helical structure of a scaffold nucleoporin and it showed an unexpected, atypical α-helical topology (Jeudy and Schwartz, 2007; Schrader et al., 2008). The 30 helices of the ~65 kDa domain, excluding the ~200 N-terminal coiled-coil domain, are arranged in a J-like topology, forming an oblong domain. The chain starts in the middle of the elongated domain, zig-zags up on one side of the molecule, folds back over a stretch of 7 helices and then continues past the N terminus to the other end of the molecule (Figures 4, 5). Three other α-helical scaffold nucleoporins (Nup84, Nup85 and Nup145C) have since been structurally characterized and shown to adopt the same fold as Nic96, pointing to a common ancestor (Brohawn et al., 2008; see below). A second, distinct α-helical fold has been identified in structures of Nup133 and Nup170, which are more distantly related, but share an extended and stretched α-helical stack (Boehmer et al., 2008; Whittle and Schwartz, 2009), substantially different from the first group. The third was revealed in the structure of Nup120, which forms a domain that fully integrates a β-propeller with an α-helical domain (Leksa et al., 2009). The α-helical segment is built around a central stalk of two long helices wrapped with 9 additional helices in an unprecedented fashion. In summary, the α-helical domains that occur in the NPC fall in different classes that provide a significant challenge for structure prediction methods. One obvious challenge is the exceedingly low sequence conservation, even between orthologs, apparent in the inconsistent nucleoporin nomenclature. Poor sequence conservation is likely due to some degree of malleability of the scaffold structure and the construction from common sequence elements (Aravind et al., 2006). Whether poor sequence conservation is further the result of adaptive evolution, linking several architectural nucleoporins to speciation, is an intriguing possibility that should be explored in more detail (Presgraves et al., 2003; Tang and Presgraves, 2009).

ACE1 Domains

As mentioned above, the four α-helical scaffold nucleoporins Nic96, Nup145C, Nup85, and Nup84 are constructed around a common ~65 kDa domain composed of 28 helices. Notably, this domain has to date only been identified outside the NPC in Sec31, one of the main building blocks of the COPII vesicle coat. The commonality was surprising. Sequence conservation between the five members is so low that no specific structural relationship was inferred previously (Alber et al., 2007, Hsia et al., 2007). This domain, which we termed Ancestral Coatomer Element 1 (ACE1), is a structural manifestation of the likely common origin of the NPC and the COPII vesicle coat (Devos et al., 2004). ACE1 is constructed from three modules, crown, trunk and tail, that together form an elongated molecule of ~ 140Å × 45Å × 45Å. Structural superposition of ACE1 proteins shows that individual modules are closely aligned, while differences in linkers between modules results in significant differences in their relative

orientations. These differences, as well as proteolytic susceptibility data, suggest at least modestly flexible hinges connect the modules, especially the trunk and the tail. This likely explains why all crystal constructs except for Nic96 contain either the trunk and crown (Brohawn et al., 2008; Debler et al., 2008; Hsia et al., 2007) or the tail (Boehmer et al., 2008). Even with the structural information in hand, it is difficult to find additional ACE1 proteins. Beyond a few residues conserved between orthologs, ACE1 is not characterized by a distinct sequence motif. The reason for this amazing degeneracy on the sequence level likely is that for folding the ACE1 domain only some general sequence profiles need to be satisfied. For example, helices α5, α7, α15 and α17 are typically hydrophobic, because they are incased by surrounding helices and are largely buried and solvent inaccessible. Thus, a combination of sequence profile evaluation, α-helical prediction, and overall length are currently the only indicators for the ACE1 domain. The two remaining α-helical scaffold nucleoporins without any crystallographic structural information are Nup188 and Nup192. Whether or not they belong to the ACE1 class, remains to be determined, but it appears unlikely.

Assembly

Structures of large protein assemblies are typically solved by a combination of cryo electron microscopy and x-ray crystallography (Chiu et al., 2006), exploiting the strengths of both methods. With EM-data in the 10-15 Å range, fitting of crystal structures can often be performed fairly reliably, providing in effect a composite structure at atomic resolution. In the case of the NPC, the best tomographic EM data for the full assembly does not extend beyond ~ 58 Å (Beck et al., 2007) and thus, unfortunately, does not lend itself to directly fitting the available crystal structures. A promising step toward closing the resolution gap is the recent EM reconstruction of the Y-complex at ~ 35 Å resolution, which allows at least tentative fitting of crystal structures (Kampmann and Blobel, 2009). Apart from the resolution gap, however, the biggest difficulty currently is the absence of strong experimental data on how the subcomplexes, notably the Y-complex, assemble to form the core scaffold structure of the NPC.

In an alternative approach to the hybrid method of combining experimental EM-and crystallographic data, Alber et al. used a plethora of volumetric and stoichiometric data, combined with distance restraints obtained from a comprehensive co-immunoprecipitation analysis of all nucleoporins, to solve the subcomplex assembly puzzle (Alber et al., 2007a; Alber et al., 2007b). Even though each datapoint has very limited information content by itself, a useful three-dimensional model is generated by combining all the data, conceptually similar to the way an NMR stucture is computed. The resulting draft model at an estimated 5 nm resolution provides a plausible arrangement of Nups in the yeast NPC, information that is not available from the current tomographic studies. According to the computed model, 8 Y-complexes each self-assemble into a cytoplasmic and a nucleoplasmic ring, defining the Z-dimension of the scaffold at ~38 nm (Figure 6). Sandwiched between the two rings are two 8-membered rings of Nup157/170,Nup188 and Nup192. All remaining nucleoporins, except for the filamentous nuclear basket and cytoplasmic extensions, have been positioned as well and decorate the main scaffold. Clearly, this model has severe limitations and will have to be adjusted with more detailed information becoming available. For instance, the Y-complex is modeled as a compact rod in the computer model and the coat is space-filling with very small gaps, both in apparent contrast to results from crystallographic analyses. The exciting possibility of this combinatorial approach however is that it should be possible to integrate currently available and forthcoming high-resolution structures to further refine the model. To date, crystal structures accounting for 23% of the mass of the NPC scaffold are available. Integration of this data could potentially reveal an NPC structure that would come fairly close to the reality.

Blobel and coworkers have taken a different experimental approach to address the subcomplex assembly problem. Their rationale is that the subcomplexes assemble only at very high protein concentrations as they are found in the assembled NPC in the living cell. Such conditions are difficult to reproduce *in vitro*, but they can potentially be mimicked in protein crystals where the protein concentration is similarly very high. Thus, crystal-packing interactions between dimeric subcomplex fragments have been used to develop an assembly model for the NPC (Debler et al., 2008; Hsia et al., 2007). Besides the overall dimensions of the scaffold, the resulting model is drastically different from the Alber model. Four instead of two 8-membered rings of Y-complexes are stacked on top of each other to form a continuous membrane-proximal shell. The rings are connected by alternating heterooctameric poles of Nup145C•Sec13 and Nup85•Seh1 (Figure 6A). The Nic96 complex is postulated to form a second, inner shell within the NPC that connects to the FG-network. Similar to the Alber model, the Y-complexes are envisioned to directly contact the pore membrane via membrane-inserting ALPS-motif containing amphipathic helices predicted to be present in several Y-complex components (Drin et al., 2007). However, experimental evidence supporting membrane-insertion is so far only available for an ALPS-helix found in the vertebrate Nup133 β-propeller, and the prediction of ALPS-helices is non-trivial. Indeed, several predicted ALPS-helices have been found to be well packed and to contribute to the hydrophobic core of nucleoporins (for example in Nup85 and Nup120), making their involvement in membrane-insertion unlikely.

Comparison to Vesicle Coats

In a groundbreaking paper, it was postulated that the NPC and vesicle coats share a common ancestor, dating back more than one billion years to the very early eukaryote (Devos et al., 2004). The principal hypothesis was that these assemblies are used to fulfill similar roles specific to eukaryotes, namely stabilizing the highly curved membranes of vesicles and the circular openings in the nuclear envelope. Judged by primary sequence analysis, however, the relationship between the components is largely undetectable. One important pillar of the 'proto-coatomer' hypothesis is that Sec13 is a bona fide component of both the COPII vesicle coat and the NPC. Structural evidence supporting the hypothesis was provided by showing that a class of four scaffold nucleoporins shares a specific 65 kDa domain, ACE1, with Sec31 of the COPII vesicle coat (Brohawn et al., 2008; Brohawn and Schwartz, 2009). The COPII coat is organized into a membrane-proximal inner layer built from Sec23•Sec24 heterodimers and Sar1, and an outer coat assembled from Sec13•Sec31 heterodimers (Stagg et al., 2008). Sec31 in the COPII coat and Nup145C in the NPC interact very similarly with Sec13 by insertion of a 7^{th} blade to complete the β-propeller. This interaction mode is recapitulated in Nup85 binding to the Sec13 homolog Seh1, which is also facilitated by insertion-completion of the β-propeller. Since Nup145C, Nup85 and Sec31 all share the same ACE1 domain, the structural data not only suggests a common ancestor, but it also provides clues as to how the NPC assembles.

In comparison to the NPC, the COPII vesicle coat is much simpler, has been extensively studied, and its assembly is quite well understood. Most informative with respect to the NPC assembly is the organization of the Sec13•Sec31 outer coat of COPII. Here, two Sec13•Sec31 heterodimers dock via their ACE1 crown modules to form an edge element (Fath et al., 2007). Four edge elements converge in a vertex, where the N-terminal β-propellers of Sec31 interact. COPII vesicles of different sizes can be assembled from different numbers of edge elements by adjusting the angles at the interaction sites (Stagg et al., 2008). In analogy to the Sec31•Sec31 homodimer interface in the COPII coat, it was predicted on a biochemical and structural basis that Nup145C and Nup84 form a heterodimeric edge element via a crown-to-crown interface in the NPC. Due to the predicted steric conflicts, this arrangement would be fundamentally incompatible with the hetero-octameric pole model discussed above (for details, see Brohawn et al., 2008). We predict that the entire NPC scaffold has an open, lattice-like organization with significant similarity to the COPII coat, also built from vertex and edge

elements (Figure 6C). As much as COPII and clathrin lattices seem not to share common construction principles (Fath et al., 2007), so do similarities between NPC and clathrin lattices not extend beyond superficial characteristics.

One important distinction between the computational and the hetero-octameric pole model on one hand and the lattice model on the other is that in the latter the Y-complex and likely also the Nic96 complex components Nic96 and Nup157/170 do not directly coat the membrane, although there may be punctual contacts. By analogy to the Sec23•Sec24 inner coat of COPII, adaptor molecules instead are predicted to directly contact the pore membrane. The transmembrane Nups, especially Ndc1, are prime candidates for this function. Indeed, Ndc1 has already been shown to physically interact with the Nic96 complex via Nup53/59 (Onischenko et al., 2009). Ndc1 is found in all eukaryotes and is essential, though this could also be related to its additional role in the spindle pole body (Winey et al., 1993). Such adaptor-mediated anchoring to the pore membrane is consistent with the membrane-proximal gaps observed in cryo-tomographic reconstructions (Beck et al., 2007; Stoffler et al., 2003).

Obviously, there are some important limitations to the analogy to COPII. First, it is not yet apparent how the verteces are formed in the NPC. In COPII, Sec31 contains an additional N-terminal β-propeller, absent in the ACE1 domains of the NPC, but essential for COPII vertex assembly (Fath et al., 2007). Thus, the vertex might look different in the NPC. Further, the COPII coat is a self-enclosed lattice structure that completely encapsulates the positively-curved membrane vesicle. In the NPC, the lattice can be continuous in lateral direction around the central transport gate, but must terminate on the nucleo- and cytoplasmic side. Further, the circular pore opening has positive curvature only in the axial direction, but negative curvature in equatorial direction. Since all vesicle coats seamlessly wrap positively curved membranes, it is not unreasonable to speculate that a specific architectural element might occur exclusively in the NPC to establish its unique geometrical requirements.

Outlook

Progress toward the structural characterization of the NPC at high resolution, one of the holy grails of structural biology (Bhattacharya, 2009), has been spectacular since our last review on the subject, a review that was intended as a roadmap toward this ambitious goal (Schwartz, 2005). The past 5 years have seen improvement in images of the entire NPC available, and a flurry of crystal structures of various key parts of the NPC. New computational methods were developed to integrate geometric data from diverse sources, and these were applied to the NPC, in part to demonstrate a general means to tackle other large assemblies (Alber et al., 2008). The path toward a high-resolution structure of the NPC will continue to be highly interdisciplinary. Single-particle reconstruction on subcomplexes has still been used only sparingly, but holds great promise to close the gap between the resolutions provided by crystallography and by tomography. It is likely that integration of structural data, particularly crystallographic data, into computationally derived models will provide further useful information. Finally, developments in super-resolution microscopy promise to allow *in vivo* measurement of distances within the NPC on the order of 10 nm, a potential source of further useful parameters – parameters so far inaccessible experimentally. These distances would complement other available structural data. Judging by recent progress in the field, dramatic developments in our understanding of the NPC lie just around the corner.

Acknowledgments

We are grateful to Elena Kiseleva and Ohad Medalia for providing images for Figure 1. Thanks to all members of the Schwartz laboratory for discussion and suggestions. We sincerely apologize to those whose work we have not referenced as a result of unintentional oversight. T.U.S. is supported by the Pew Scholars Program and by NIH grant GM077537.

References

Akey CW, Radermacher M. Architecture of the Xenopus nuclear pore complex revealed by three-dimensional cryo-electron microscopy. J. Cell Biol 1993;122:1–19. [PubMed: 8314837]

Akhtar A, Gasser SM. The nuclear envelope and transcriptional control. Nat. Rev. Genet 2007;8:507–517. [PubMed: 17549064]

Alber F, Dokudovskaya S, Veenhoff LM, Zhang W, Kipper J, Devos D, Suprapto A, Karni-Schmidt O, Williams R, Chait BT, et al. Determining the architectures of macromolecular assemblies. Nature 2007a;450:683–694. [PubMed: 18046405]

Alber F, Dokudovskaya S, Veenhoff LM, Zhang W, Kipper J, Devos D, Suprapto A, Karni-Schmidt O, Williams R, Chait BT, et al. The molecular architecture of the nuclear pore complex. Nature 2007b; 450:695–701. [PubMed: 18046406]

Alber F, Forster F, Korkin D, Topf M, Sali A. Integrating diverse data for structure determination of macromolecular assemblies. Annu. Rev. Biochem 2008;77:443–477. [PubMed: 18318657]

Antonin W, Ellenberg J, Dultz E. Nuclear pore complex assembly through the cell cycle: regulation and membrane organization. FEBS Lett 2008;582:2004–2016. [PubMed: 18328825]

Aravind L, Iyer LM, Koonin EV. Comparative genomics and structural biology of the molecular innovations of eukaryotes. Curr. Opin. Struct. Biol 2006;16:409–419. [PubMed: 16679012]

Bailer SM, Balduf C, Hurt E. The Nsp1p carboxy-terminal domain is organized into functionally distinct coiled-coil regions required for assembly of nucleoporin subcomplexes and nucleocytoplasmic transport. Mol. Cell Biol 2001;21:7944–7955. [PubMed: 11689687]

Bayliss R, Littlewood T, Stewart M. Structural basis for the interaction between FxFG nucleoporin repeats and importin-beta in nuclear trafficking. Cell 2000;102:99–108. [PubMed: 10929717]

Beck M, Lucic V, Forster F, Baumeister W, Medalia O. Snapshots of nuclear pore complexes in action captured by cryo-electron tomography. Nature 2007;449:611–615. [PubMed: 17851530]

Belgareh N, Snay-Hodge C, Pasteau F, Dagher S, Cole CN, Doye V. Functional characterization of a Nup159p-containing nuclear pore subcomplex. Mol. Biol. Cell 1998;9:3475–3492. [PubMed: 9843582]

Berke IC, Boehmer T, Blobel G, Schwartz TU. Structural and functional analysis of Nup133 domains reveals modular building blocks of the nuclear pore complex. J. Cell Biol 2004;167:591–597. [PubMed: 15557116]

Bhattacharya A. Protein structures: Structures of desire. Nature 2009;459:24–27. [PubMed: 19424134]

Boehmer T, Enninga J, Dales S, Blobel G, Zhong H. Depletion of a single nucleoporin, Nup107, prevents the assembly of a subset of nucleoporins into the nuclear pore complex. Proc. Natl. Acad. Sci. U S A 2003;100:981–985. [PubMed: 12552102]

Boehmer T, Jeudy S, Berke IC, Schwartz TU. Structural and functional studies of Nup107/Nup133 interaction and its implications for the architecture of the nuclear pore complex. Mol. Cell 2008;30:721–731. [PubMed: 18570875]

Brohawn SG, Leksa NC, Spear ED, Rajashankar KR, Schwartz TU. Structural evidence for common ancestry of the nuclear pore complex and vesicle coats. Science 2008;322:1369–1373. [PubMed: 18974315]

Brohawn SG, Schwartz TU. A lattice model of the nuclear pore complex. Comm. Integr. Biol 2009;2:1–3.

Carmody SR, Wente SR. mRNA nuclear export at a glance. J. Cell Sci 2009;122:1933–1937. [PubMed: 19494120]

Chaudhuri I, Soding J, Lupas AN. Evolution of the beta-propeller fold. Proteins 2008;71:795–803. [PubMed: 17979191]

Chiu W, Baker ML, Almo SC. Structural biology of cellular machines. Trends Cell Biol 2006;16:144–150. [PubMed: 16459078]

Cook A, Bono F, Jinek M, Conti E. Structural biology of nucleocytoplasmic transport. Annu. Rev. Biochem 2007;76:647–671. [PubMed: 17506639]

Cronshaw JM, Krutchinsky AN, Zhang W, Chait BT, Matunis MJ. Proteomic analysis of the mammalian nuclear pore complex. J. Cell Biol 2002;158:915–927. [PubMed: 12196509]

D'Angelo MA, Hetzer MW. Structure, dynamics and function of nuclear pore complexes. Trends Cell Biol 2008;18:456–466. [PubMed: 18786826]

D'Angelo MA, Raices M, Panowski SH, Hetzer MW. Age-dependent deterioration of nuclear pore complexes causes a loss of nuclear integrity in postmitotic cells. Cell 2009;136:284–295. [PubMed: 19167330]

Daigle N, Beaudouin J, Hartnell L, Imreh G, Hallberg E, Lippincott-Schwartz J, Ellenberg J. Nuclear pore complexes form immobile networks and have a very low turnover in live mammalian cells. J. Cell Biol 2001;154:71–84. [PubMed: 11448991]

Debler EW, Ma Y, Seo HS, Hsia KC, Noriega TR, Blobel G, Hoelz A. A fence-like coat for the nuclear pore membrane. Mol. Cell 2008;32:815–826. [PubMed: 19111661]

Devos D, Dokudovskaya S, Alber F, Williams R, Chait BT, Sali A, Rout MP. Components of coated vesicles and nuclear pore complexes share a common molecular architecture. PLoS Biol 2004;2:e380. [PubMed: 15523559]

Devos D, Dokudovskaya S, Williams R, Alber F, Eswar N, Chait BT, Rout MP, Sali A. Simple fold composition and modular architecture of the nuclear pore complex. Proc. Natl. Acad. Sci. U S A 2006;103:2172–2177. [PubMed: 16461911]

Drin G, Casella JF, Gautier R, Boehmer T, Schwartz TU, Antonny B. A general amphipathic alpha-helical motif for sensing membrane curvature. Nat. Struct. Mol. Biol 2007;14:138–146. [PubMed: 17220896]

Dultz E, Zanin E, Wurzenberger C, Braun M, Rabut G, Sironi L, Ellenberg J. Systematic kinetic analysis of mitotic dis- and reassembly of the nuclear pore in living cells. J. Cell Biol 2008;180:857–865. [PubMed: 18316408]

Edeling MA, Smith C, Owen D. Life of a clathrin coat: insights from clathrin and AP structures. Nat. Rev. Mol. Cell. Biol 2006;7:32–44. [PubMed: 16493411]

Elad N, Maimon T, Frenkiel-Krispin D, Lim RY, Medalia O. Structural analysis of the nuclear pore complex by integrated approaches. Curr. Opin. Struct Biol 2009;19:226–232. [PubMed: 19327984]

Fabre E, Hurt E. Yeast genetics to dissect the nuclear pore complex and nucleocytoplasmic trafficking. Annu. Rev. Genet 1997;31:277–313. [PubMed: 9442897]

Fahrenkrog B, Aris JP, Hurt EC, Pante N, Aebi U. Comparative spatial localization of protein-A-tagged and authentic yeast nuclear pore complex proteins by immunogold electron microscopy. J. Struct. Biol 2000;129:295–305. [PubMed: 10806080]

Fath S, Mancias JD, Bi X, Goldberg J. Structure and Organization of Coat Proteins in the COPII Cage. Cell 2007;129:1325–1336. [PubMed: 17604721]

Feuerbach F, Galy V, Trelles-Sticken E, Fromont-Racine M, Jacquier A, Gilson E, Olivo-Marin JC, Scherthan H, Nehrbass U. Nuclear architecture and spatial positioning help establish transcriptional states of telomeres in yeast. Nat. Cell Biol 2002;4:214–221. [PubMed: 11862215]

Franz C, Walczak R, Yavuz S, Santarella R, Gentzel M, Askjaer P, Galy V, Hetzer M, Mattaj IW, Antonin W. MEL-28/ELYS is required for the recruitment of nucleoporins to chromatin and postmitotic nuclear pore complex assembly. EMBO Rep 2007;8:165–172. [PubMed: 17235358]

Frey S, Gorlich D. A saturated FG-repeat hydrogel can reproduce the permeability properties of nuclear pore complexes. Cell 2007;130:512–523. [PubMed: 17693259]

Fribourg S, Braun IC, Izaurralde E, Conti E. Structural basis for the recognition of a nucleoporin FG repeat by the NTF2-like domain of the TAP/p15 mRNA nuclear export factor. Mol. Cell 2001;8:645–656. [PubMed: 11583626]

Galy V, Mattaj IW, Askjaer P. Caenorhabditis elegans nucleoporins Nup93 and Nup205 determine the limit of nuclear pore complex size exclusion in vivo. Mol. Biol. Cell 2003;14:5104–5115. [PubMed: 12937276]

Grandi P, Doye V, Hurt EC. Purification of NSP1 reveals complex formation with 'GLFG' nucleoporins and a novel nuclear pore protein NIC96. EMBO J 1993;12:3061–3071. [PubMed: 7688296]

Grandi P, Schlaich N, Tekotte H, Hurt EC. Functional interaction of Nic96p with a core nucleoporin complex consisting of Nsp1p, Nup49p and a novel protein Nup57p. EMBO J 1995;14:76–87. [PubMed: 7828598]

Grant RP, Neuhaus D, Stewart M. Structural basis for the interaction between the Tap/NXF1 UBA domain and FG nucleoporins at 1A resolution. J. Mol. Biol 2003;326:849–858. [PubMed: 12581645]

Handa N, Kukimoto-Niino M, Akasaka R, Kishishita S, Murayama K, Terada T, Inoue M, Kigawa T, Kose S, Imamoto N, et al. The crystal structure of mouse Nup35 reveals atypical RNP motifs and novel homodimerization of the RRM domain. J. Mol. Biol 2006;363:114–124. [PubMed: 16962612]

Harel A, Orjalo AV, Vincent T, Lachish-Zalait A, Vasu S, Shah S, Zimmerman E, Elbaum M, Forbes DJ. Removal of a single pore subcomplex results in vertebrate nuclei devoid of nuclear pores. Mol. Cell 2003;11:853–864. [PubMed: 12718872]

Hawryluk-Gara LA, Shibuya EK, Wozniak RW. Vertebrate Nup53 interacts with the nuclear lamina and is required for the assembly of a Nup93-containing complex. Mol Biol Cell 2005;16:2382–2394. [PubMed: 15703211]

Heessen S, Fornerod M. The inner nuclear envelope as a transcription factor resting place. EMBO Rep 2007;8:914–919. [PubMed: 17906672]

Herzog F, Primorac I, Dube P, Lenart P, Sander B, Mechtler K, Stark H, Peters JM. Structure of the anaphase-promoting complex/cyclosome interacting with a mitotic checkpoint complex. Science 2009;323:1477–1481. [PubMed: 19286556]

Hinshaw JE, Carragher BO, Milligan RA. Architecture and design of the nuclear pore complex. Cell 1992;69:1133–1141. [PubMed: 1617726]

Hodel AE, Hodel MR, Griffis ER, Hennig KA, Ratner GA, Xu S, Powers MA. The three-dimensional structure of the autoproteolytic, nuclear pore-targeting domain of the human nucleoporin Nup98. Mol. Cell 2002;10:347–358. [PubMed: 12191480]

Hsia KC, Stavropoulos P, Blobel G, Hoelz A. Architecture of a coat for the nuclear pore membrane. Cell 2007;131:1313–1326. [PubMed: 18160040]

Jeudy S, Schwartz TU. Crystal structure of nucleoporin Nic96 reveals a novel, intricate helical domain architecture. J. Biol. Chem 2007;282:34904–34912. [PubMed: 17897938]

Kalverda B, Fornerod M. The nuclear life of nucleoporins. Dev. Cell 2007;13:164–165. [PubMed: 17681127]

Kampmann M, Blobel G. Three-dimensional structure and flexibility of a membrane-coating module of the nuclear pore complex. Nat. Struct. Mol. Biol 2009;16:782–788. [PubMed: 19503077]

Kiseleva E, Allen TD, Rutherford S, Bucci M, Wente SR, Goldberg MW. Yeast nuclear pore complexes have a cytoplasmic ring and internal filaments. J. Struct. Biol 2004;145:272–288. [PubMed: 14960378]

Kiseleva E, Goldberg MW, Cronshaw J, Allen TD. The nuclear pore complex: structure, function, and dynamics. Crit. Rev. Eukaryot. Gene Expr 2000;10:101–112. [PubMed: 10813398]

Kobe B, Kajava AV. When protein folding is simplified to protein coiling: the continuum of solenoid protein structures. Trends Biochem. Sci 2000;25:509–515. [PubMed: 11050437]

Kohler A, Hurt E. Exporting RNA from the nucleus to the cytoplasm. Nat. Rev. Mol. Cell. Biol 2007;8:761–773. [PubMed: 17786152]

Kosova B, Pante N, Rollenhagen C, Hurt E. Nup192p is a conserved nucleoporin with a preferential location at the inner site of the nuclear membrane. J. Biol. Chem 1999;274:22646–22651. [PubMed: 10428845]

Kramer A, Ludwig Y, Shahin V, Oberleithner H. A pathway separate from the central channel through the nuclear pore complex for inorganic ions and small macromolecules. J. Biol. Chem 2007;282:31437–31443. [PubMed: 17726020]

Leksa NC, Brohawn SG, Schwartz TU. The structure of the scaffold nucleoporin Nup120 reveals a new and unexpected domain architecture. Structure *epub*. 2009

Li SJ, Hochstrasser M. The yeast ULP2 (SMT4) gene encodes a novel protease specific for the ubiquitin-like Smt3 protein. Mol. Cell. Biol 2000;20:2367–2377. [PubMed: 10713161]

Lim RY, Fahrenkrog B, Koser J, Schwarz-Herion K, Deng J, Aebi U. Nanomechanical basis of selective gating by the nuclear pore complex. Science 2007;318:640–643. [PubMed: 17916694]

Lim RY, Ullman KS, Fahrenkrog B. Biology and biophysics of the nuclear pore complex and its components. Int. Rev. Cell. Mol. Biol 2008;267:299–342. [PubMed: 18544502]

Liu SM, Stewart M. Structural basis for the high-affinity binding of nucleoporin Nup1p to the Saccharomyces cerevisiae importin-beta homologue, Kap95p. J. Mol. Biol 2005;349:515–525. [PubMed: 15878174]

Lutzmann M, Kunze R, Buerer A, Aebi U, Hurt E. Modular self-assembly of a Y-shaped multiprotein complex from seven nucleoporins. EMBO J 2002;21:387–397. [PubMed: 11823431]

Makio T, Stanton LH, Lin CC, Goldfarb DS, Weis K, Wozniak RW. The nucleoporins Nup170p and Nup157p are essential for nuclear pore complex assembly. J. Cell Biol 2009;185:459–473. [PubMed: 19414608]

Matsuoka Y, Takagi M, Ban T, Miyazaki M, Yamamoto T, Kondo Y, Yoneda Y. Identification and characterization of nuclear pore subcomplexes in mitotic extract of human somatic cells. Biochem. Biophys. Res. Commun 1999;254:417–423. [PubMed: 9918853]

Melcak I, Hoelz A, Blobel G. Structure of Nup58/45 suggests flexible nuclear pore diameter by intermolecular sliding. Science 2007;315:1729–1732. [PubMed: 17379812]

Napetschnig J, Blobel G, Hoelz A. Crystal structure of the N-terminal domain of the human protooncogene Nup214/CAN. Proc. Natl. Acad. Sci. U S A 2007;104:1783–1788. [PubMed: 17264208]

Nehrbass U, Rout MP, Maguire S, Blobel G, Wozniak RW. The yeast nucleoporin Nup188p interacts genetically and physically with the core structures of the nuclear pore complex. J. Cell Biol 1996;133:1153–1162. [PubMed: 8682855]

Onischenko E, Stanton LH, Madrid AS, Kieselbach T, Weis K. Role of the Ndc1 interaction network in yeast nuclear pore complex assembly and maintenance. J. Cell Biol 2009;185:475–491. [PubMed: 19414609]

Paoli M. Protein folds propelled by diversity. Prog. Biophys. Mol. Biol 2001;76:103–130. [PubMed: 11389935]

Partridge JR, Schwartz TU. Crystallographic and Biochemical Analysis of the Ran-binding Zinc Finger Domain. J. Mol. Biol 2009;391:375–389. [PubMed: 19505478]

Pemberton LF, Paschal BM. Mechanisms of receptor-mediated nuclear import and nuclear export. Traffic 2005;6:187–198. [PubMed: 15702987]

Peters R. Translocation through the nuclear pore: Kaps pave the way. Bioessays 2009;31:466–477. [PubMed: 19274657]

Powell L, Burke B. Internuclear exchange of an inner nuclear membrane protein (p55) in heterokaryons: in vivo evidence for the interaction of p55 with the nuclear lamina. J. Cell Biol 1990;111:2225–2234. [PubMed: 2277058]

Presgraves DC, Balagopalan L, Abmayr SM, Orr HA. Adaptive evolution drives divergence of a hybrid inviability gene between two species of Drosophila. Nature 2003;423:715–719. [PubMed: 12802326]

Pryer NK, Salama NR, Schekman R, Kaiser CA. Cytosolic Sec13p complex is required for vesicle formation from the endoplasmic reticulum in vitro. J. Cell Biol 1993;120:865–875. [PubMed: 8432727]

Rabut G, Doye V, Ellenberg J. Mapping the dynamic organization of the nuclear pore complex inside single living cells. Nat. Cell Biol 2004;6:1114–1121. [PubMed: 15502822]

Rasala BA, Orjalo AV, Shen Z, Briggs S, Forbes DJ. ELYS is a dual nucleoporin/kinetochore protein required for nuclear pore assembly and proper cell division. Proc. Natl. Acad. Sci. U S A 2006;103:17801–17806. [PubMed: 17098863]

Reichelt R, Holzenburg A, Buhle EL Jr. Jarnik M, Engel A, Aebi U. Correlation between structure and mass distribution of the nuclear pore complex and of distinct pore complex components. J. Cell Biol 1990;110:883–894. [PubMed: 2324201]

Rout MP, Aitchison JD, Magnasco MO, Chait BT. Virtual gating and nuclear transport: the hole picture. Trends Cell. Biol 2003;13:622–628. [PubMed: 14624840]

Rout MP, Aitchison JD, Suprapto A, Hjertaas K, Zhao Y, Chait BT. The yeast nuclear pore complex: composition, architecture, and transport mechanism. J. Cell Biol 2000;148:635–651. [PubMed: 10684247]

Rout MP, Blobel G. Isolation of the yeast nuclear pore complex. J. Cell Biol 1993;123:771–783. [PubMed: 8227139]

Schrader N, Koerner C, Koessmeier K, Bangert JA, Wittinghofer A, Stoll R, Vetter IR. The crystal structure of the Ran-Nup153ZnF2 complex: a general Ran docking site at the nuclear pore complex. Structure 2008a;16:1116–1125. [PubMed: 18611384]

Schrader N, Stelter P, Flemming D, Kunze R, Hurt E, Vetter IR. Structural basis of the nic96 subcomplex organization in the nuclear pore channel. Mol. Cell 2008b;29:46–55. [PubMed: 18206968]

Schwartz TU. Modularity within the architecture of the nuclear pore complex. Curr. Opin. Struct. Biol 2005;15:221–226. [PubMed: 15837182]

Siniossoglou S, Lutzmann M, Santos-Rosa H, Leonard K, Mueller S, Aebi U, Hurt E. Structure and assembly of the Nup84p complex. J. Cell Biol 2000;149:41–54. [PubMed: 10747086]

Stagg SM, LaPointe P, Razvi A, Gurkan C, Potter CS, Carragher B, Balch WE. Structural basis for cargo regulation of COPII coat assembly. Cell 2008;134:474–484. [PubMed: 18692470]

Stewart M. Molecular mechanism of the nuclear protein import cycle. Nat. Rev. Mol. Cell. Biol 2007;8:195–208. [PubMed: 17287812]

Stoffler D, Feja B, Fahrenkrog B, Walz J, Typke D, Aebi U. Cryo-electron tomography provides novel insights into nuclear pore architecture: implications for nucleocytoplasmic transport. J. Mol. Biol 2003;328:119–130. [PubMed: 12684002]

Strambio-de-Castillia C, Blobel G, Rout MP. Proteins connecting the nuclear pore complex with the nuclear interior. J. Cell Biol 1999;144:839–855. [PubMed: 10085285]

Sun Y, Guo HC. Structural constraints on autoprocessing of the human nucleoporin Nup98. Protein Sci 2008;17:494–505. [PubMed: 18287282]

Tang S, Presgraves DC. Evolution of the Drosophila nuclear pore complex results in multiple hybrid incompatibilities. Science 2009;323:779–782. [PubMed: 19197064]

Terry LJ, Wente SR. Nuclear mRNA export requires specific FG nucleoporins for translocation through the nuclear pore complex. J. Cell. Biol 2007;178:1121–1132. [PubMed: 17875746]

Tran EJ, Wente SR. Dynamic nuclear pore complexes: life on the edge. Cell 2006;125:1041–1053. [PubMed: 16777596]

Vetter IR, Nowak C, Nishimoto T, Kuhlmann J, Wittinghofer A. Structure of a Ran-binding domain complexed with Ran bound to a GTP analogue: implications for nuclear transport. Nature 1999;398:39–46. [PubMed: 10078529]

von Moeller H, Basquin C, Conti E. The mRNA export protein DBP5 binds RNA and the cytoplasmic nucleoporin NUP214 in a mutually exclusive manner. Nat. Struct. Mol. Biol 2009;16:247–254. [PubMed: 19219046]

Walther TC, Alves A, Pickersgill H, Loiodice I, Hetzer M, Galy V, Hulsmann BB, Kocher T, Wilm M, Allen T, et al. The conserved Nup107-160 complex is critical for nuclear pore complex assembly. Cell 2003;113:195–206. [PubMed: 12705868]

Watson ML. Further observations on the nuclear envelope of the animal cell. J. Biophys. Biochem. Cytol 1959;6:147–156. [PubMed: 13843146]

Weirich CS, Erzberger JP, Berger JM, Weis K. The N-terminal domain of Nup159 forms a beta-propeller that functions in mRNA export by tethering the helicase Dbp5 to the nuclear pore. Mol. Cell 2004;16:749–760. [PubMed: 15574330]

Weis K. Regulating access to the genome: nucleocytoplasmic transport throughout the cell cycle. Cell 2003;112:441–451. [PubMed: 12600309]

Whittle JR, Schwartz TU. Architectural nucleoporins Nup157/170 and Nup133 are structurally related and descend from a second ancestral element. J. Biol. Chem. pub. 2009

Winey M, Hoyt MA, Chan C, Goetsch L, Botstein D, Byers B. NDC1: a nuclear periphery component required for yeast spindle pole body duplication. J Cell Biol 1993;122:743–751. [PubMed: 8349727]

Xu Y, Xing Y, Chen Y, Chao Y, Lin Z, Fan E, Yu JW, Strack S, Jeffrey PD, Shi Y. Structure of the protein phosphatase 2A holoenzyme. Cell 2006;127:1239–1251. [PubMed: 17174897]

Zuleger N, Korfali N, Schirmer EC. Inner nuclear membrane protein transport is mediated by multiple mechanisms. Biochem. Soc. Trans 2008;36:1373–1377. [PubMed: 19021558]

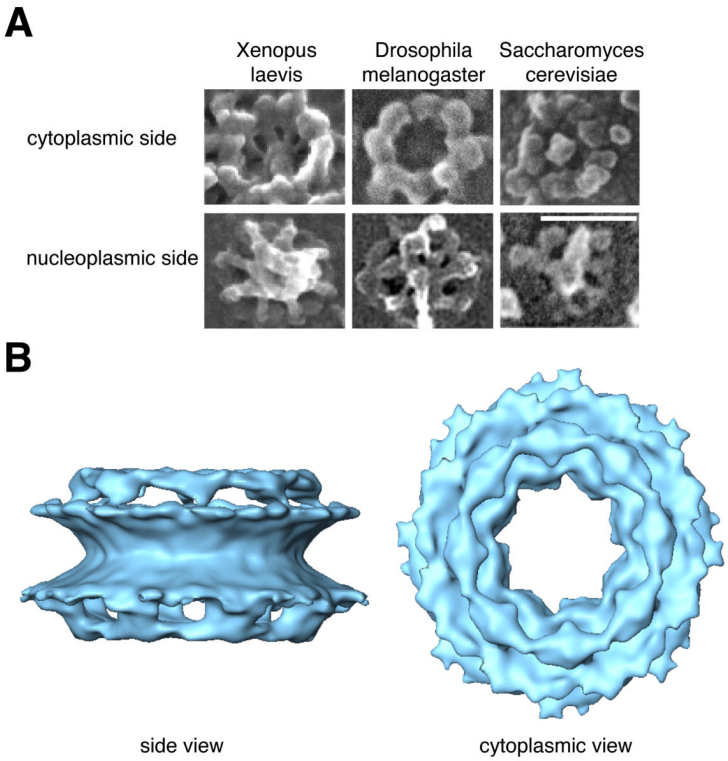

Figure 1. Overall Structure of the Nuclear Pore Complex

(A) Representative micrographs of NPCs from diverse eukaryotes and obtained by scanning electron microscopy. The distinct surface features that define cytoplasmic and nucleoplasmic face of the NPC are conserved, so are the overall dimensions in the plane of the nuclear envelope. Scale bar indicates 100nm.

(B) Cryo-electron tomographic (cryo-ET) reconstruction of the human NPC. The nuclear basket structure and the cytoplasmic extensions are omitted for clarity. The central eightfold rotational symmetry is clearly visible. A comparison between cryo-ET reconstructions of NPCs from diverse species reveals substantial differences in the overall height (Elad et al., 2009).

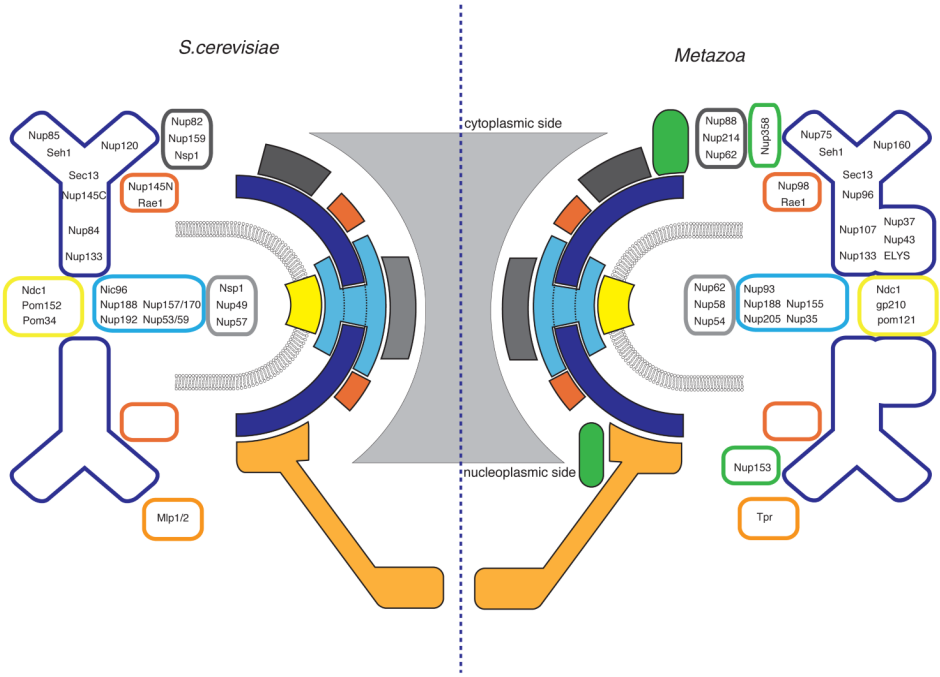

Figure 2. Schematic Representation of the Modular Assembly of the NPC

The NPC is built from ~30 nucleoporins, organized in a small set of subcomplexes. The cartoon shows the major subcomplexes that make up the lattice-like scaffold (blue colors), the membrane-attachment (yellow), and the FG-network (grey) of the NPC. S.cerevisiae components on the left, metazoa, with specific additional components on the right. A few peripheral nups are left out for clarity. Simplified representation, connections are not to be taken literally and box sizes are not proportional to molecular weights.

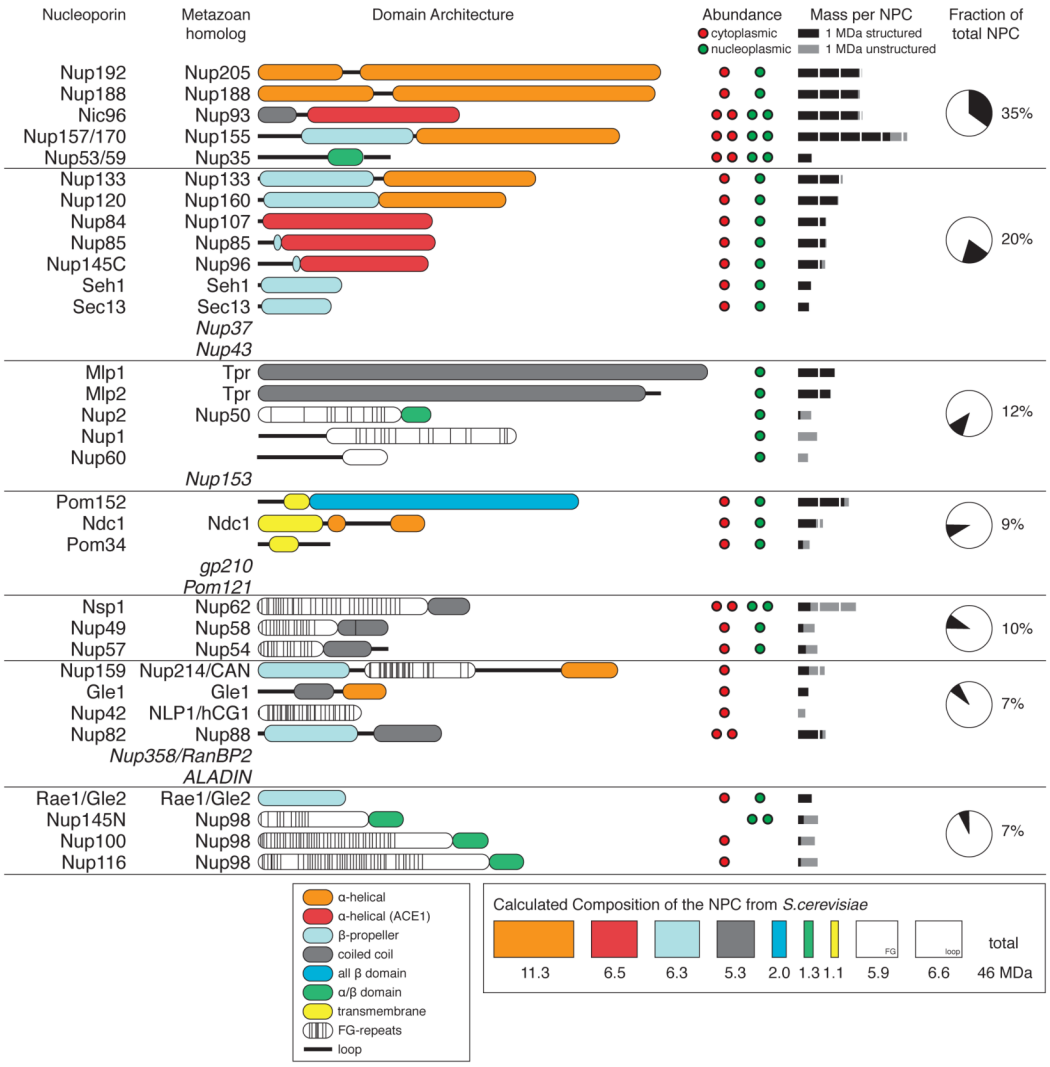

Figure 3. Inventory of the NPC

Summary of the nucleoporins that make up the NPC. Domain architecture of nucleoporins from S.cerevisiae as determined by x-ray crystallography or prediction (where structural information is still lacking). Abundance and derived mass calculations are based on published Nup/NPC stoichiometries (Rout et al., 2000; Cronshaw et al., 2003). Nucleoporins specific to metazoa are italicized.

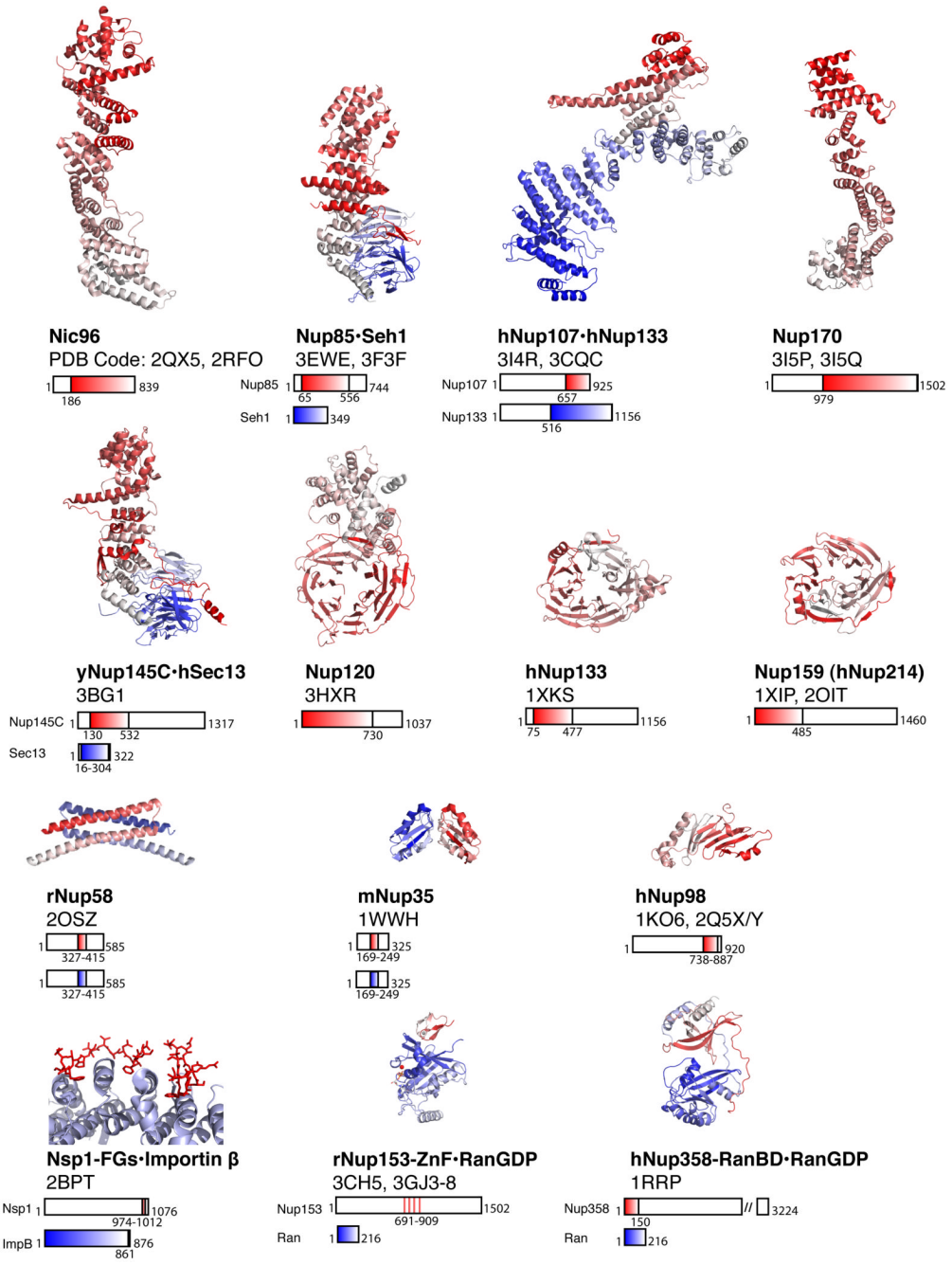

Figure 4. Structures of Nucleoporins

Comprehensive list of all representative nucleoporin structures published to date. PDB accession codes are indicated. Structures are gradient-colored red- or blue-to-white from N to C terminus. Residue information for each crystallized fragment are given below the structure. Structures are shown in the assembly state that is supported by crystallographic and biochemical evidence. Structures are from S.cerevisiae unless noted otherwise (h, human; m,mouse; r, rat). 2QX5(Jeudy and Schwartz, 2007); 2RFO(Schrader et al., 2008b); 3EWE (Brohawn et al., 2008); 3F3F(Debler et al., 2008); 3CQC(Boehmer et al., 2008) 3I4R, 3I5P, 3I5Q(Whittle and Schwartz, 2009), 3BG1(Hsia et al., 2007); 3HXR(Leksa et al., 2009); 1XKS (Berke et al., 2004); 1XIP(Weirich et al., 2004); 2OIT(Napetschnig et al., 2007); 2OSZ(Melcak

et al., 2007); 1WWH(Handa et al., 2006); 1KO6(Hodel et al., 2002); 2Q5X/Y(Sun and Guo, 2008); 2BPT(Liu and Stewart, 2005); 3CH5(Schrader et al., 2008a); 3GJ3-8(Partridge and Schwartz, 2009); 1RRP(Vetter et al., 1999).

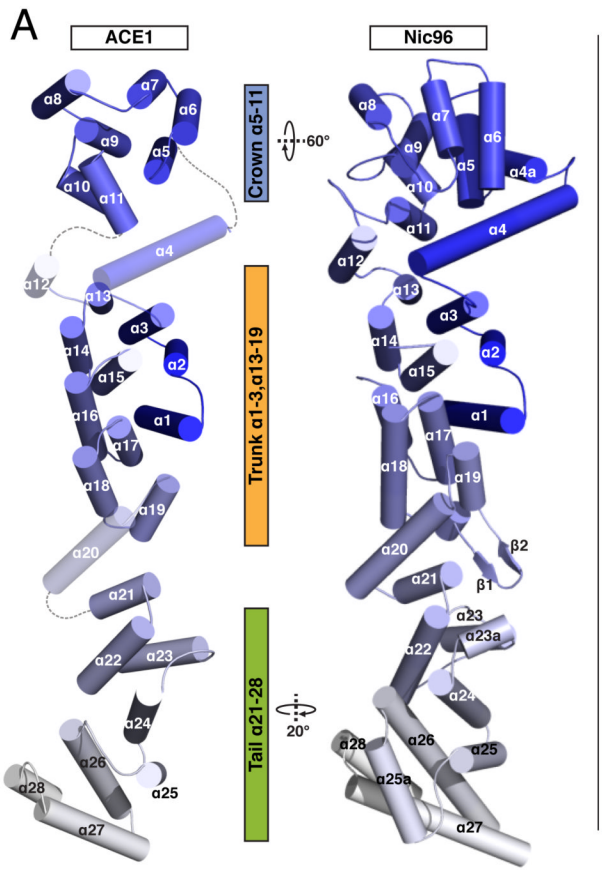

B

ACE1 helix	Nic96	Nup145C	Nup85	Nup84	Sec31
1	205-228	188-196	103-117	n.d.	417-424
2	234-243	217-223	134-164	35-54	428-435
3	248-263	229-242	170-188	60-84	441-455
4	270-294	253-287	201-212	114-129	459-462
5	333-343	290-301	244-253	171-190	510-519
6	345-356	304-314	257-266	192-203	524-531
7	366-373	317-326	280-292	206-218	536-543
8	388-396	331-346	300-317	240-253	549-560
9	406-416	352-363	326-339	258-268	568-577
10	426-430	373-379	343-348	273-277	582-586
11	432-442	382-392	354-362	282-305	594-603
12	457-469	399-410	372-381	324-335	608-624
13	478-485	417-427	390-398	342-352	628-638
14	486-498	431-441	406-411	354-368	642-660
15	500-513	447-460	415-427	386-404	666-685
16	534-543	469-485	462-475	409-422	697-712
17	550-562	488-497	480-491	n.d.	717-724
18	566-583	501-514	497-509	n.d.	731-744
19	586-611	526-530	517-528	n.d.	n.d.
20	617-634	534-553	532-543	n.d.	n.d.
21	637-647	n.d.	n.d.	667- 680	n.d.
22	650-667	n.d.	n.d.	686-700	n.d.
23	685-697	n.d.	n.d.	705-723	n.d.
24	708-728	n.d.	n.d.	739-768	n.d.
25	732-742	n.d.	n.d.	783- 820	n.d.
26	765-790	n.d.	n.d.	841-867	n.d.
27	800-820	n.d.	n.d.	871-882	n.d.
28	826-835	n.d.	n.d.	895-913	n.d.

Figure 5. The Ancestral Coatomer Element ACE1

Four scaffold nucleoporins, Nic96, Nup85, Nup84, and Nup145C share a distinct 65 kDa domain also found in the COPII protein Sec31, manifesting common evolutionary ancestry between the two membrane coats. (Devos et al., 2004; Brohawn et al., 2008). (A) The structures of an “average” ACE1 protein (left) and Nic96 (right) are shown in cartoon form and colored from blue (N-terminus) to white (C-terminus). The regions corresponding to the crown, trunk, and tail modules are indicated. The “average” ACE1 protein was made for illustrative purposes by superimposing the known ACE1 protein structures crown, trunk, and tail modules separately and constructing each of the 28 helices and connecting loops in the most frequently observed position. The orientation of the modules with respect to one another is shown in the average ACE1 case to most clearly show the architecture and connectivity of the fold. The position of the crown and tail modules in Nic96 are rotated 60° and 20° respe ctively compared to the average ACE1 structure as indicated. **(B)** The amino acid assignment for each of the canonical 28 ACE1 helices is indicated for all structurally characterized ACE1 proteins. All numbering is from *S. cerevisiae* except for helices 21-28 from Nup84, which correspond the human homolog Nup107. Helices are colored according to the module to which they belong as are the labels in **(A)**. n.d. (not determined) indicates helices that fall within regions of the proteins for which no structural information is available.

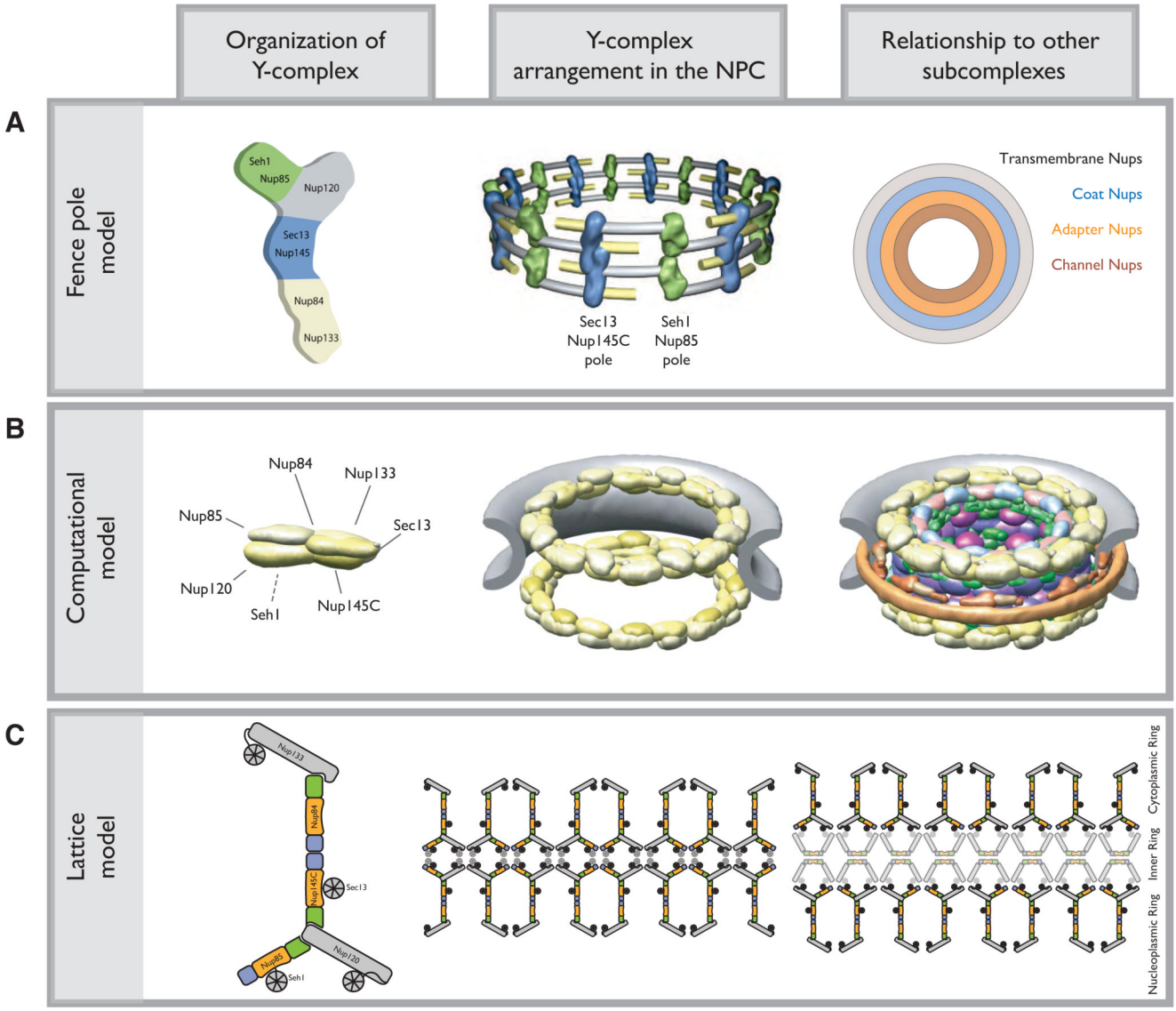

Figure 6. Assembly Models for the NPC

Three recently proposed models for the structural organization of the NPC are illustrated. The fence pole model (top row), computationally generated model (middle row), and lattice model (bottom row) are compared in their prediction of protein interactions within one Y-complex (left column), Y-complex organization within the NPC (middle column), and placement of Y-complexes relative to other NPC subcomplexes (right column). In the fence pole model, heterooctameric poles of Nup145C•Sec13 and Nup85•Seh1 observed in crystal structures organize four rings of 8 Y-complexes each. These four rings form a cylinder adjacent to the transmembrane Nups on the membrane side and layers of adaptor Nups followed by channel Nups towards the transport channel (Hsia et al., 2007; Debler et al., 2008). The computationally generated model provides localization volumes for each Nup and shows 8 Y-complexes arranged into two separate rings, one towards the nucleocytoplasmic and the other the cytoplasmic side of the NPC. The other Nups are arranged into membrane rings, inner rings, linkers between rings, and FG nucleoporins (Alber et al., 2007). The lattice model is based on structural homology of ACE1 proteins in the NPC and COPII vesicle coat (Brohawn et al., 2008). ACE1 proteins are colored by module with tails green, trunks orange, and crowns blue.

A model of a single Y-complex incorporates the demonstrated specific interactions between domains of the 7 proteins. 8 Y-complexes are assumed to form a nucleoplasmic and cytoplasmic ring, which may or may not be connected by additional lattice elements such as Nic96 and Nup157/170 in an inner ring. The illustration is meant to emphasize the predicted open, lattice-like organization of the NPC structural scaffold and is not meant to imply specific interactions between complexes. While it seems likely that the NPC lattice will be composed of ACE1-containing edge elements and vertex elements made from β-propeller interactions as observed in the COPII vesicle coat, the exact nature of the vertex elements in the NPC lattice remains to be seen (Brohawn et al., 2008).